Magneto-optical observation of dynamic relaxation in $YBa_2Cu_3O_{7-\delta}$ thin films

1997 J. Phys.: Condens. Matter 9 10909

(http://iopscience.iop.org/0953-8984/9/49/010)

J. Phys.: Condens. Matter **9** (1997) 10909–10918. Printed in the UK PII: S0953-8984(97)87360-2

Magneto-optical observation of dynamic relaxation in $YBa_2Cu_3O_{7-\delta}$ thin films

M R Koblischka†‖, T H Johansen†, H Bratsberg†, L Půst‡¶, Y Shen§ and P Vase§

† Department of Physics, University of Oslo, Blindern, N-0316 Oslo, Norway
‡ Institute of Physics, Academy of Sciences of the Czech Republic, Na Slovance 2, CZ-18040 Praha 8, Czech Republic
§ Nordic Superconductor Technologies A/S, Priorparken 878, DK-2605 Brøndby, Denmark

Received 5 September 1997

Abstract. Using magneto-optical visualization of the flux in superconductors, the dependence of the flux distributions on the rate of sweep of the external magnetic field $\mathrm{d}H_{\mathrm{ext}}/\mathrm{d}t$ ('dynamic relaxation') is directly observed for $YBa_2Cu_3O_{7-\delta}$ thin films patterned into small rectangles. The differences in the flux patterns are clearly detectable especially when the sample is not fully penetrated. Various ways of analysing the flux patterns in order to determine the dynamic relaxation rate Q quantitatively from the magneto-optical images are discussed.

1. Introduction

One of the outstanding features of high-T_c superconductors is the very strong time dependence of their magnetization (flux creep) [1]. This time dependence of the magnetization is known as flux creep or 'giant' flux creep and can be described by the flux creep equation [2–5]. The understanding and control of flux creep is of great importance for future applications of high-T_c superconductors, and, at the same time, it is an interesting phenomenon for theoretical study. Vortex systems can be studied by various methods; the most widely used ones are measurements of the magnetic moments caused by induced superconducting currents under various conditions. While these magnetic measurements give global information about the gradients of the vortex density averaged over the sample, the *direct* magneto-optical observations show the *local* distributions of the flux. Using the magneto-optical visualization techniques based on the Faraday effect which combine a relatively high spatial resolution with the unique possibility of observing dynamic processes [6–9] with a good time resolution [10], a direct observation of flux creep effects can be realized. Such local observations of creep effects are of great importance, enabling a comparison of the shape of the spatial flux distribution during the relaxation process with theory to be made. Furthermore, the influence of defects within the sample on the creep behaviour can be studied directly, which is important also for applications of the high-T_c materials, as the control of flux creep is still a crucial open problem. The local observation technique allows also a quantitative analysis to be made of creep data even for samples

‖ Also at: Department of Physics, NTNU Trondheim, N-7034 Trondheim, Norway.
¶ Present address: Department of Physics and Astronomy, Wayne State University, 666 W Hancock, Detroit, MI 48202, USA.

0953-8984/97/4910909+10$19.50

with inhomogeneous current distributions; see, e.g., the analysis of creep data for partly heavy-ion-irradiated high-T_c single crystals [11].

As far as we are aware, all magneto-optical investigations of flux creep published up to now were performed while keeping the external magnetic field at a constant value ('conventional relaxation'). Successful experiments were carried out on single crystals, thin films and even on individual grains of granular superconductors [9, 11–13]. However, the flux creep equation [2–5] provides the basis for another way of performing a flux creep experiment. This experiment is carried out by measuring magnetization loops with various rates of sweep of the external magnetic field. The separation between these loops is a direct measure for the change in current density depending on the sweep rate, $\mathrm{d}H_{\mathrm{ext}}/\mathrm{d}t$. The corresponding creep rate, Q, is called the dynamic relaxation rate. This method proved to be very useful for measuring relaxation processes at short relaxation times [4, 14–16], mainly for thin superconductors [15].

In this paper we will show that the differences in the flux patterns produced by using different sweep rates to reach a given final field value can be directly observed using magneto-optics. As the sample, we have chosen a $YBa_2Cu_3O_{7-\delta}$ (YBCO) thin film patterned into a rectangular shape. This sample shows an excellent quality without any defects disturbing the flux patterns [17], thus enabling a direct comparison of our results with theory to be made. Furthermore, we will discuss various possibilities for quantitatively obtaining the dynamic relaxation rate, Q, depending on the geometry of the experiment, on the sample shape and on the magnetic conditions.

This paper is organized as follows. In section 2, we will outline the differences between conventional and dynamic relaxations. In section 3, we give a short description of the magneto-optical technique and the experimental details. In section 4, the results obtained for an YBCO thin film are discussed. Furthermore, various techniques for obtaining the dynamic creep rate Q are discussed and compared to each other. Finally, in section 5, some conclusions are drawn.

2. Theoretical background

The particular distribution of magnetic flux in a superconducting sample, i.e. the structure of the vortex system, depends on the field history and on the relaxation in the vortex system. Relaxation processes in superconductors can be described by the flux creep equation [2–5]

$$\Omega\mu_0\frac{\mathrm{d}j}{\mathrm{d}t} = -\chi_0\frac{\mathrm{d}H_{\mathrm{ext}}}{\mathrm{d}t} + \Delta v_0\frac{B_{\mathrm{int}}}{\mu_0}P(j,T,B_{\mathrm{int}}). \tag{1}$$

The differential susceptibility χ_0 and the geometric factor Δ depend on the size and shape of the sample. $\Omega = M/j$ denotes the proportionality factor of j and the magnetization M, v_0 denotes the vortex velocity and B_{int} denotes the internal field. $P(j,T,B_{\mathrm{int}})$ denotes the vortex hopping probability. Over a wide temperature range (typically from 10 K up to temperatures close to the irreversibility line) the dynamics of the vortices is governed by the regime of thermally activated flux motion (TAFM), where $P(j,T,B_{\mathrm{int}})$ is proportional to $\exp[-U/kT]$, where $U(j,T,B_{\mathrm{int}})$ is a current-, temperature- and field-dependent effective activation energy. However, at very low temperatures ($T \approx 2$ K and below) vortices predominantly tunnel through a pinning barrier [5, 18].

The structure of equation (1) leads directly to two different ways of performing a flux creep experiment.

(i) The external magnetic field H_{ext} is swept to a given target value, and kept constant there, and the time dependence of the magnetic moment or another quantity reflecting the time decay of the superconducting currents is recorded. This process is called 'relaxation creep' or conventional relaxation (CR, $dH_{ext}/dt = 0$) [2, 19].

(ii) Various field cycles are measured, but using different rates of sweep dH_{ext}/dt of the external magnetic field to reach an identical final field value. This experiment is referred to as dynamic relaxation or 'sweep creep' (DR, $dH_{ext}/dt \neq 0$) [4, 14, 15, 19].

The CR and DR techniques give complementary information about $P(j, T, B_{int})$, but for different ranges of parameters. In the case of DR the vortex motion probability P is directly proportional to the field sweep rate as $P = (\chi_0/\Delta v_0 B_{int})(dB_{ext}/dt)$, while during CR experiments P continuously changes with time t. As follows from equation (1), the superconducting currents in a sample can be calculated as soon as $P(j, T, B_{int})$ is specified.

From the experimental point of view, a DR flux creep experiment is more favourable because there is no problem with the definition of the starting time of the relaxation experiment like that in CR experiments. The DR technique also avoids effects like field over- and undershoots produced by the magnet which can heavily influence the results [15].

DR flux creep experiments are based on the fact that the flux has relaxed already *during* the sweep of the external magnetic field. This implies that the gradients of the flux (vortex density) are larger when the external magnetic field is swept quickly and the gradients are smaller when lower sweep rates are used as the vortex system has more time to relax into states closer to equilibrium. Consequently, the difference between the flux at a given place in the sample and the flux at the circumference of the sample is smaller for lower sweep rates (deeper penetration) and larger for larger sweep rates (less deep penetration). Using low rates of field sweeping enables the vortices to relax along the flux density gradients thus leading to a deeper penetration. In a former publication [4], it was shown that this method of measuring various hysteresis loops with different sweep rates is well suited for investigating fast relaxation effects. For this reason, dynamic relaxations are mostly measured by means of magnetometers with short recording times, typically via vibrating-sample magnetometry or the torque magnetometers [3, 4, 14, 15].

3. Experimental procedure

The magneto-optical (MO) visualization techniques are described in detail in references [6, 7]. The field distribution is obtained via the Faraday effect, i.e. the rotation of the plane of polarization of linearly polarized light which passes a magneto-optically active layer exposed to the magnetic field of the underlying superconductor. From flux-free regions the light is reflected without rotation, and thus cannot pass the analyser which is set in a crossed position with respect to the polarizer. In this way, the flux-line lattice is imaged as bright areas, whereas the flux-free Meissner area stays dark. The images presented here are, therefore, maps of the z-component of the local magnetic field, B_z.

The magneto-optical technique has two outstanding advantages: one of them is that it allows one to also observe dynamic processes in the vortex lattice; the other is that it provides the possibility of performing experiments over a wide range of length scales, i.e. from whole samples down to individual grains. The spatial resolution of the MO technique depends on the type of indicator used in the experiment; see the recent review article on MO flux visualization (reference [7]). As the magneto-optical active layer, here we have used a Bi-doped yttrium iron garnet (YIG) film with in-plane anisotropy. The thickness of the active layer is 4 μm, half of which corresponds to the spatial resolution of our experiment. The images are recorded using an 8-bit Kodak DCS 420 CCD digital camera (1536 $\times$ 1024 pixels per frame) and subsequently transferred to a computer for

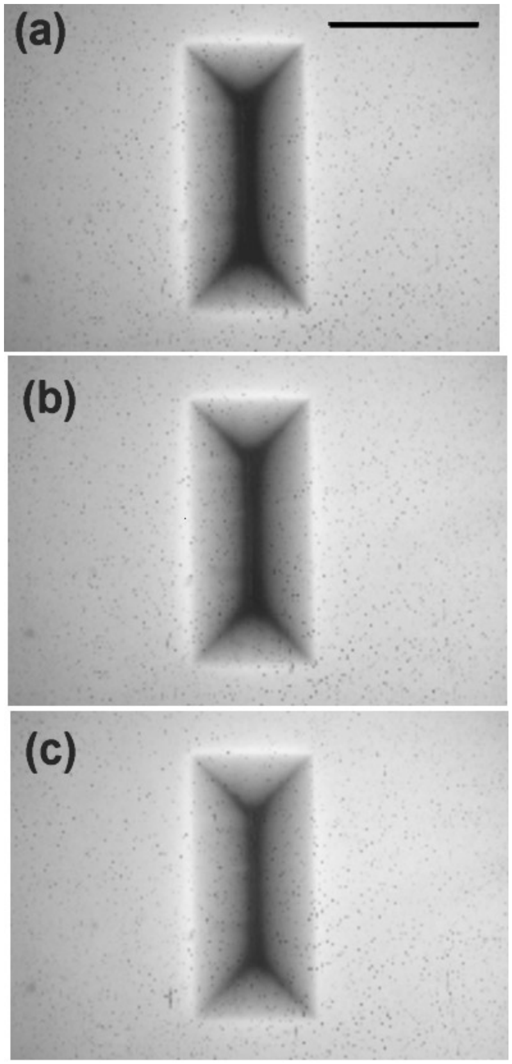

Figure 1. Flux distributions on a rectangularly patterned YBCO thin film, obtained at $T = 18$ K. The marker is 1 mm long. Note the excellent quality of the sample which is entirely free of structural defects, thus allowing a direct comparison to the theoretical calculations of flux distributions. The external magnetic field is swept in all images to $\mu_0 H_{ext} = 50$ mT, but using different sweep rates $\mathrm{d}H_{ext}/\mathrm{d}t$: (a) 10 mT s^{-1}; (b) 1.6 mT s^{-1}; and (c) 0.2 mT s^{-1}. It is clearly visible that a slow sweep rate leads to a deeper penetration of the flux. All of these experiments were started from a zero-field-cooled virgin state.

processing. Unless otherwise stated, the exposure time of the camera is always set to 1 s.

Thin films of $YBa_2Cu_3O_{7-\delta}$ were made by laser ablation on a MgO substrate. The sample had a thickness of 200 nm, and a transition temperature of 89.8 K. More details of the sample preparation can be found in reference [20]. The rectangular shape was formed by etching, resulting in a size of 660×1400 μm^2. In the MO apparatus the sample was mounted on the cold finger of an optical helium-flow cryostat [7, 8, 21] using a thermally conductive carbon cement (‘CCC’ [22]) ensuring a good thermal contact.

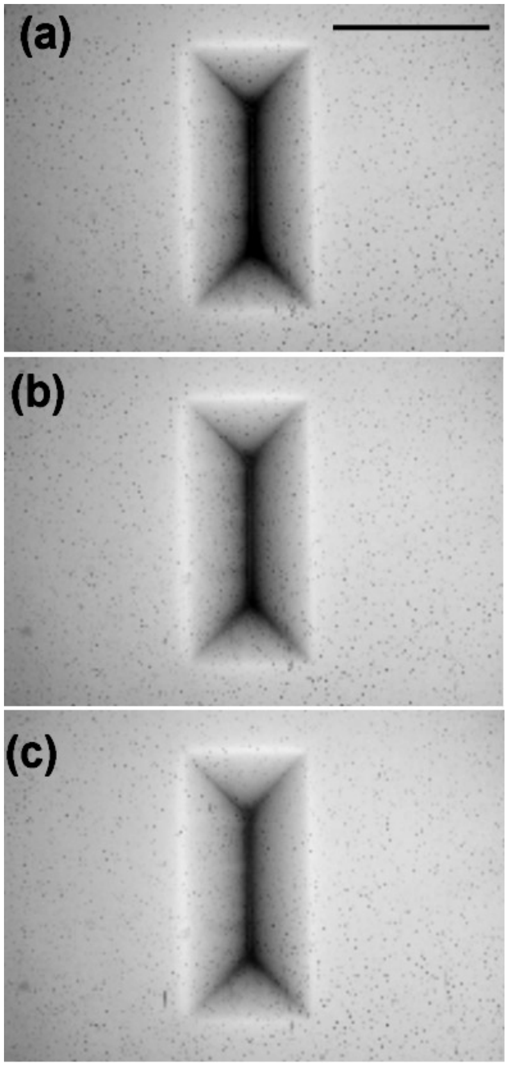

Figure 2. Flux distributions obtained on the same sample as in figure 1 but at $T = 40$ K; the final field value is now always 40 mT. The magnetic field is swept at different sweep rates $\mathrm{d}H_{\mathrm{ext}}/\mathrm{d}t$: (a) 10 mT s^{-1}; (b) 1.6 mT s^{-1}; and (c) 0.2 mT s^{-1}. These sweep rates are identical to those in figure 1. The larger degree of relaxation at the higher temperature is clearly visible.

The magnetic field was applied perpendicularly to the film plane using a copper solenoid coil with a maximum field of ± 120 mT. A DR flux creep experiment requires the use of a programmable power supply enabling the magnet to keep a constant sweep rate $\mathrm{d}H_{\mathrm{ext}}/\mathrm{d}t$.

4. Results and discussion

In figures 1(a)–1(c), we present a DR experiment at $T = 18$ K and the flux structure is recorded always at $\mu_0 = 50$ mT. The sweep rates range from 10 mT s^{-1} (a), through 1.6 mT s^{-1} (b) to 0.2 mT s^{-1} (c). The rectangular thin film used in this experiment proves to be of excellent quality without any defects disturbing the flux patterns [17]. This enables

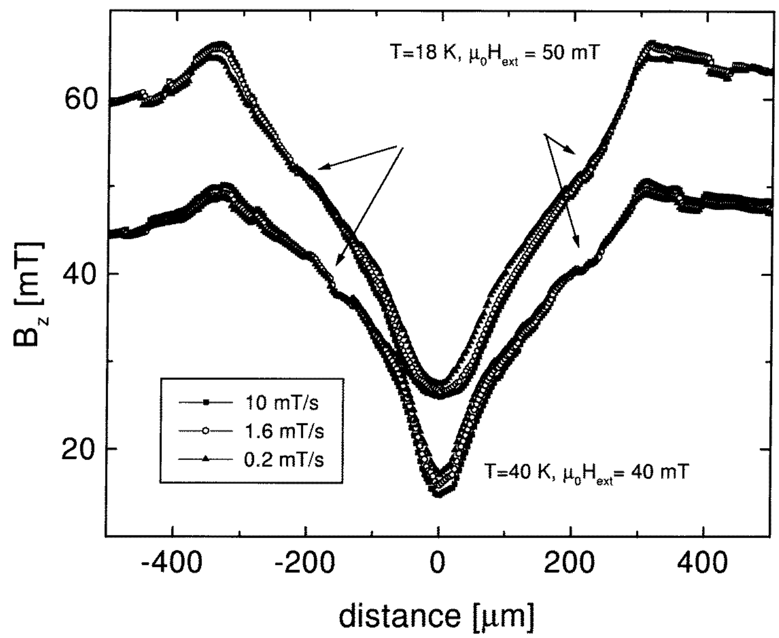

Figure 3. Flux density profiles read across the sample centre; $x = 0$ denotes the centreline of the sample. The neutral line with no flux creep is clearly visible as the crossing point of the three corresponding flux profiles (marked by arrows). This demonstrates that the *local* relaxation depends strongly on the position within the sample.

a direct comparison of the MO images to the theoretical calculations of flux profiles in perpendicular geometry to be made [23–25]. At this relatively low temperature and small fields, the influence of the sweep rate on the flux patterns can already been seen quite clearly from the amount of Meissner phase residing at the centre of the sample. The slower the sweep rate during the sweep up to the target field, the smaller the flux gradients measured in the sample. If the pinning potential, U, of the sample is quite small, then very homogeneous flux patterns may be formed when sweeping the magnetic field slowly. It is important to point out that all of these subsequent experiments were started from a completely virgin state, i.e. after each experimental run the sample is warmed up to a temperature $T > T_c$ while keeping all of the optical settings in a fixed position. This was done in order to compare these results with ones obtained by the procedure used in magnetometry, where the so-called minor hysteresis loops (hysteresis loops measured around a given central-field value) are measured starting with the fastest sweep rate and, subsequently, the sweep rate is reduced after each loop (see, e.g., the measurements presented in references [14–16]). The MO flux distributions prove that these two procedures yield identical results.

Figures 2(a)–2(c) present a similar experiment at $T = 40$ K. The sweep rates are identical to those in figure 1; the final field value is now 40 mT. This observation clearly reveals the enhanced relaxation, and the effect of the sweep rate on the flux distribution is more pronounced here; at a sweep rate of 0.2 mT s^{-1} we have already come close to a fully penetrated state.

In figure 3, the corresponding flux density profiles are shown, read across the sample centre. The profiles are reflecting directly the decay of the superconducting current density,

j_s, with time or sweep rate, i.e. $j_s = f(t, \mathrm{d}H_{ext}/\mathrm{d}t)$. The flux profiles also show *where* in the sample the flux is moving during a relaxation experiment.

In perpendicular geometry, the characteristic field overshoot at the sample edges is decaying during the sweep and, simultaneously, flux is penetrating deeper into the sample. This implies that the relaxation process is strongly dependent on the position within the sample, as locally regions with an increasing amount of flux and a decreasing amount of flux can be found. This observation, however, does not imply that the resulting creep rate Q can be positive or negative [26] as the creep rate depends only on the change in current density.

In reference [27], the existence of a neutral line which is not affected during a relaxation process defined by $B_z(x, y) = \mu_0 H_{ext}$ was predicted, and this was observed in references [9, 28]. This neutral line also exists in a dynamic creep experiment. The position of the discontinuity lines of the currents [29] (i.e. where the currents flowing along the sample edges are forced to make a sharp turn) is not affected during the relaxation process, as these lines depend only on the sample geometry. However, if the pinning potential of the sample is small, then very homogeneously distributed flux patterns may result when a slow sweep rate is used. It is also important to note that all of the characteristic field values, such as the full penetration field, H^*, are strongly dependent on the sweep rates of the magnetic field used in the experiment. This is especially important when the results obtained by means of magneto-optics are compared to data obtained by other techniques. The flux profiles taken at $T = 40$ K reveal the enhanced relaxation due to the lowered pinning potential; in particular, the flux penetration during creep into the Meissner region is more pronounced.

The MO investigations allow us to also determine the flux creep rate quantitatively from the images. The dynamic creep rate, Q, is defined as

$$Q = \mathrm{d}\ln j_s/\mathrm{d}\ln(\mathrm{d}H_{ext}/\mathrm{d}t) \tag{2}$$

so Q depends only on the superconducting current density. This implies that the change of the current density with time has to be determined from the MO images. The feasibility of this task depends strongly on the geometry of the experiment, on the shape of the sample investigated and on the magnetic state.

In longitudinal geometry, corresponding to the critical-state model in its original form as given by Bean [30], Kim *et al* [31], and others, j_s can be directly obtained from the measured flux density gradients. For high-T_c samples the case of perpendicular geometry is, however, more important, as we are mostly dealing with flat, small samples (thin films, tapes etc) with H_{ext} oriented perpendicular to the sample surface. Therefore, an inversion procedure has to be applied in order to reconstruct j_s from the MO images [32].

For determining Q quantitatively from the magneto-optical patterns, there are several different methods, depending on the state of flux penetration and the sample shape.

(i) If the sample is free of macroscopic defects and has a simple regular shape, i.e. takes the form of a thin, long strip, a rectangle or a circle, the measured flux density profiles can be fitted using the models for calculation of current distributions and flux profiles in perpendicular geometry (the field applied perpendicular to the sample surface) developed recently [23–25]. In a more general case, a reconstruction of the current flow by means of an inversion procedure [32] has to be carried out. From the current densities, Q can be obtained by plotting $\ln j_s$ versus $\ln(\mathrm{d}H_{ext}/\mathrm{d}t)$. This procedure is identical to the treatment of data obtained by magnetometry. Moreover, the knowledge of the particular flux distribution throughout the sample at various rates of the field sweep provides unique information which cannot be extracted from the *integral* magnetic measurements. In principle, this is partly comparable to measurements using sets of microscopic Hall probes [26]; however, the MO technique provides a much larger number of ‘sensors’ (pixels) to analyse. Procedure (i) is ideally suited for quantitative determinations of Q by means of magneto-optics.

(ii) For an irregular sample shape, or a defect-containing, but not fully penetrated sample, the width of the Meissner area, b, or the width of the flux front, w (for a thin strip $w = a - b$, with a denoting the width of the strip) is a measure of the current density and, therefore, of the relaxation regarding the differences in b of two subsequent states. The relation between the differences in b obtained in a DR experiment and the currents j_s can be directly verified from the flux profiles calculated either in the perpendicular geometry [23, 24], e.g. $b = a/\cosh(\pi B_{ext}/\mu_0 j_s)$, or in the longitudinal geometry. This method of analysis is practical if the rate of creep of the flux at a defect in the sample is studied. Q can then be obtained via a logarithmic plot of the differences in w versus $\ln(\mathrm{d}H_{ext}/\mathrm{d}t)$. For a state that is not fully penetrated in a sample with regular shape, method (ii) is the same as method (i).

(iii) For irregular sample shape, or defects and an arbitrary state of flux penetration, the magneto-optical visualization also offers a very general way of analysing the flux patterns by studying the total intensity, I_{tot}, in a given frame (or throughout the whole image), which is a measure of the flux, Φ. In former publications [9, 11], magneto-optical CR experiments were analysed in this way. This treatment implies summing all of the intensities measured within a given frame to obtain the total intensity I_{tot}, which is a function of the external magnetic field H_{ext}, the sweep rate $\mathrm{d}H_{ext}/\mathrm{d}t$ and the temperature T, e.g. $I_{tot} = f(H_{ext}, \mathrm{d}H_{ext}/\mathrm{d}t, T)$. The variation of I_{tot} with the sweep rate is obvious directly from the images presented in figures 1 and 2. A plot of I_{tot} versus $\ln \mathrm{d}H_{ext}/\mathrm{d}t$ yields then a measure of Q. This allows Q to be determined also at defects or in samples with inhomogeneous current distributions, by choosing the frame for the analysis appropriately. The analysis of I_{tot} is not influenced by the sample geometry; in the extreme case, simply the whole image can be used to work with. As a recorded digitized image contains in our case 1536 $\times$ 1024 pixels to analyse, *local* relaxations can be studied in great detail. Such an analysis of local flux creep in homogeneous and defect-containing samples will be presented elsewhere [33].

The near-perfect sample used in this experiment enables a comparison between these different methods to be made. Applying method (i) to the flux profiles presented in figure 3 yields $Q = 0.021$ ($T = 18$ K, $\mu_0 H_{ext} = 50$ mT) and $Q = 0.032$ ($T = 40$ K, $\mu_0 H_{ext} = 40$ mT). Method (ii) yields the same results as (i), as can be directly verified from the flux profiles shown in figure 3. The integration method (iii) gives $Q = 0.022$ ($T = 18$ K, $\mu_0 H_{ext} = 50$ mT) and $Q = 0.035$ ($T = 40$ K, $\mu_0 H_{ext} = 40$ mT) with a frame just enclosing the sample. This comparison shows the validity of the different methods, thus opening several possibilities to observe locally flux creep effects by magneto-optics.

5. Conclusions

In conclusion, we have demonstrated the dependence of the flux distributions obtained by magneto-optical visualization techniques on the rate of sweep of the external magnetic field. Direct observations and measurements of the flux creep are now possible for both modes predicted by the flux creep equation. Several possible ways of analysing the flux patterns in order to obtain the dynamic relaxation rate Q are discussed. The magneto-optical techniques for visualization of the flux enable further a *local* determination of the dynamic rate of creep, Q, at defect structures or for samples within inhomogeneous current distributions to be carried out.

Acknowledgments

We acknowledge valuable discussions with M Jirsa (Academy of Sciences of the Czech Republic, Prague) and R Wijngaarden and R Griessen (Free University, Amsterdam). This work was financially supported by The Research Council of Norway; the work in Prague was supported by grant No A1010512 of GA ASCR.

References

[1] Müller K A, Takashige M and Bednorz J G 1987 *Phys. Rev. Lett.* **58** 1143
Blatter G, Geshkenbein V B and Vinokur V M 1991 *Phys. Rev. Lett.* **66** 3297
[2] Hagen C W and Griessen R 1989 *Studies of High Temperature Superconductors* vol 3, ed A Narlikar (New York: Nova Science) p 159
[3] Schnack H G, Griessen R, Lensink J G, van der Beek C J and Kes P H 1992 *Physica* C **197** 337
[4] Jirsa M, Půst L, Schnack H G and Griessen R 1993 *Physica* C **207** 85
[5] Půst L, Martinez J C, Griessen R, Jirsa M, van Dalen A J J, Hoekstra A, Wen H H and Ravi Kumar G 1994 *Critical Currents in Superconductors* ed H W Weber (Singapore: World Scientific) p 240
[6] Hübener R P 1979 *Magnetic Flux Structures in Superconductors (Springer Series in Solid State Sciences 6)* (Berlin: Springer)
[7] Koblischka M R and Wijngaarden R J 1995 *Supercond. Sci. Technol.* **8** 199
[8] Indenbom M V, Koleshnikov N N, Kulakov M P, Naumenko I G, Nikitenko V I, Polyanskii A A, Vershinin N F and Vlasko-Vlasov V K 1990 *Physica* C **166** 486
[9] Koblischka M R, Schuster T, Ludescher B and Kronmüller H 1992 *Physica* C **190** 557
[10] The time resolution of the magneto-optical techniques can range from several seconds down to nanoseconds; see, e.g.,
Leiderer P, Boneberg J, Brüll P, Bujok V and Herminghaus S 1994 *Phys. Rev. Lett.* **71** 2646
[11] Schuster T, Leghissa M, Koblischka M R, Kuhn H, Kronmüller H, Kraus M and Saemann-Ischenko G 1992 *Physica* C **203** 203
Schuster T, Koblischka M R, Kuhn H, Kronmüller, Leghissa M, Gerhäuser W, Saemann-Ischenko G, Neumüller H W and Klaumünzer S 1992 *Phys. Rev.* B **46** 8496
[12] Muller H, Suenaga M and Yokoyama Y 1991 *J. Appl. Phys.* **70** 4409
[13] Forkl A, Habermeier H-U, Knorpp R, Theuss H and Kronmüller H 1993 *Physica* C **211** 121
[14] Půst L, Kadlecova J, Jirsa M and Durcok S 1990 *J. Low Temp. Phys.* **78** 179
[15] van Dalen A J J, Koblischka M R and Griessen R 1996 *Physica* C **259** 157
[16] van Dalen A J J, Griessen R and Koblischka M R 1996 *Physica* C **257** 271
[17] Koblischka M R 1996 *Supercond. Sci. Technol.* **9** 271
[18] Caldeira A O and Leggett A J 1981 *Phys. Rev. Lett.* **46** 211
[19] Caplin A D, Cohen L F, Perkins G K and Zhukov A A 1994 *Supercond. Sci. Technol.* **7** 412
[20] Vase P, Shen Y and Freltoft T 1991 *Physica* C **180** 90
[21] Johansen T H, Baziljevich M, Bratsberg H, Galperin Y, Lindelof P E, Shen Y and Vase P 1996 *Phys. Rev.* B **54** 16 264
[22] 'Conductive carbon cement' (CCC), from Neubauer Chemikalien, D-48031 Münster, Germany.
[23] Brandt E H and Indenbom M V 1993 *Phys. Rev.* B **48** 12 893
Brandt E H 1993 *Phys. Rev. Lett.* **71** 2821
Brandt E H 1994 *Phys. Rev.* B **49** 9024
Schuster T, Kuhn H, Brandt E H, Indenbom M V, Koblischka M R and Konczykowski M 1994 *Phys. Rev.* B **50** 16 684
[24] Zeldov E, Clem J R, McElfresh M and Darwin M 1994 *Phys. Rev.* B **49** 9802
[25] McDonald J and Clem J R 1996 *Phys. Rev.* B **53** 8643
[26] Abulafia Y, Shaulov A, Wolfus Y, Prozorov R, Burlachkov L, Yeshurun Y, Majer D, Zeldov E and Vinokur V M 1995 *Phys. Rev. Lett.* **75** 2404
Abulafia Y, Shaulov A, Wolfus Y, Prozorov R, Burlachkov L, Majer D, Zeldov E, Vinokur V M and Yeshurun Y 1997 *J. Low Temp. Phys.* **107** 455
[27] Gurevich A and Brandt E H 1994 *Phys. Rev. Lett.* **73** 178
[28] Schuster T, Kuhn H and Brandt E H 1995 *Phys. Rev.* B **51** 697
[29] Schuster T, Indenbom M V, Koblischka M R, Kuhn H and Kronmüller H 1994 *Phys. Rev.* B **49** 3443
[30] Bean C P 1962 *Phys. Rev. Lett.* **8** 250

[31] Kim Y B, Hempstead C F and Strnad A R 1962 *Phys. Rev. Lett.* **9** 306
[32] Pashitski A E, Gurevich A, Polyanskii A A, Larbalestier D C, Goyal A, Specht E D, Kroeger D M, DeLuca J A and Tkaczyk J E 1997 *Science* **275** 367
Wijngaarden R J, Spoelder H J W, Surdeanu R and Griessen R 1996 *Phys. Rev.* B **54** 6742
Johansen T H, Galperin Y and Bratsberg H 1997 *Phys. Rev.* B submitted
[33] Koblischka M R, Johansen T H, Bratsberg H, Shen Y and Vase P 1997 in preparation